Experimental Neurology 311 (2019) 67–79

Contents lists available at ScienceDirect

Experimental Neurology

journal homepage: www.elsevier.com/locate/yexnr

Research Paper

Inhibition of sphingomyelin synthase 1 ameliorates alzheimer-like pathology in APP/PS1 transgenic mice through promoting lysosomal degradation of BACE1

Mei-Hong Lu[a,b], Wen-Li Ji[a,b], De-En Xu[c], Pei-Pei Yao[a,b], Xiu-Yun Zhao[a,b], Zhao-Tao Wang[d], Li-Pao Fang[a,b], Rui Huang[a,b], Li-Jun Lan[a,b], Ji-Bo Chen[a,b], Ting-Hua Wang[e], Li-Hua Cheng[d], Ru-Xiang Xu[d], Chun-Feng Liu[a,b], Luigi Puglielli[f], Quan-Hong Ma[a,b,d,*]

[a] Jiangsu Key Laboratory of Translational Research and Therapy for Neuro-Psycho- Diseases, Institute of Neuroscience, Soochow University, Suzhou 215004, China
[b] Department of Neurology and Suzhou Clinical Research Center of Neurological Disease, the Second Affiliated Hospital of Soochow University, Suzhou 215004, China
[c] Department of Neurology, The Second People's Hospital of Wuxi, Wuxi 214002, China
[d] Affiliated Bayi Brain Hospital, Military General Hospital of Beijing PLA, Southern Medical University, Beijing 100700, China
[e] Institute of Neuroscience, Kunming Medical University, Kunming 650500, China
[f] Department of Medicine and Wisconsin Alzheimer's Disease Research Center, University of Wisconsin-Madison, Madison, WI 53705, USA

ARTICLE INFO

Keywords:
BACE1
Sphingomyelin
Amyloid-β
Lysosomal degradation
Alzheimer's disease
Lipids

ABSTRACT

Sphingolipids emerge as essential modulators in the etiology of Alzheimer's disease (AD) with unclear mechanisms. Elevated levels of SM synthase 1 (SMS1), which catalyzes the synthesis of SM from ceramide and phosphatidylcholine, have been observed in the brains of Alzheimer's disease (AD), where expression of β-site APP cleaving enzyme 1 (BACE1), a rate limiting enzyme in amyloid-β (Aβ) generation, are upregulated. In the present study, we show knockdown of SMS1 via andeno associated virus (serotype 8, AAV8) in the hippocampus of APP/PS1 transgenic mice, attenuates the densities of Aβ plaques, neuroinflammation, synaptic loss and thus rescuing cognitive deficits of these transgenic mice. We further describe that knockdown or inhibition of SMS1 decreases BACE1 stability, which is accompanied with decreased BACE1 levels in the Golgi, whereas enhanced BACE1 levels in the early endosomes and the lysosomes. The reduction of BACE1 levels induced by knockdown or inhibition of SMS1 is prevented by inhibition of lysosomes. Therefore, knockdown or inhibition of SMS1 promotes lysosomal degradation of BACE1 via modulating the intracellular trafficking of BACE1. Knockdown of SMS1 attenuates AD-like pathology through promoting lysosomal degradation of BACE1.

1. Introduction

Alzheimer's disease (AD) is a neurodegenerative disorder characterized clinically by progressive memory decline as well as aberrant behavior. Amyloid-β (Aβ), especially its oligomeric form, is the initiator to trigger the pathological processes in AD such as neuroinflammation, loss of synapses and cognitive deficits (Musiek and Holtzman, 2015; Yang et al., 2017). β-secretase (β-site APP cleaving enzyme 1, BACE1) is the rate limiting enzyme in Aβ generation, which cleaves APP together with γ-secretase to generate Aβ. BACE1-deficient neurons and AD transgenic mice produce no soluble Aβ and Aβ plaques (Cai et al., 2001; Luo et al., 2001). Mutation of APP at A673T which suppresses cleavage by BACE1 exhibits cognitive benefit in human (Jonsson et al., 2012). Therefore, inhibiting BACE1 is one of prime targets of AD therapy. It is worth noting that elevated levels and activity of BACE1 have been detected in the brains of AD patients with unclear mechanisms (Holsinger et al., 2002; Yang et al., 2003). Thus, identification of molecular pathways regulating BACE1 expression or activity may bring novel targets or strategies for AD therapy.

"Lipid granule accumulation" was originally described by Alois Alzheimer as the third hallmark of AD brain (Foley, 2010). Recent studies further reveal a close link of lipids to AD pathogenesis. A number of genes involved in lipid metabolism are genetically associated with late onset AD (Naj et al., 2011). Among them, E4 isoform of apolipoprotein E, which encodes a lipid transport protein, is the strongest genetic risk factor for AD (Bertram and Tanzi, 2008). Cholesterol, which exhibits abnormal levels in the brains of both of AD patients and transgenic mice (Walter and van Echten-Deckert, 2013),

* Corresponding author at: Block 402, Ren-Ai Road 199, Suzhou, Jiangsu 215021, China.
E-mail address: maquanhong@suda.edu.cn (Q.-H. Ma).

https://doi.org/10.1016/j.expneurol.2018.09.012
Received 5 June 2018; Received in revised form 12 August 2018; Accepted 17 September 2018
Available online 20 September 2018
0014-4886/

regulates Aβ production through modulating γ-secretase activity (Di Paolo and Kim, 2011; Walter and van Echten-Deckert, 2013). Sphingolipids, which modulates biological processes including cell growth, differentiation and senescence, shows altered levels in the brains of AD patients (van Echten-Deckert and Walter, 2012). Sphingomyelin (SM) and ceramide are two major species of sphingolipids, which can convert to each other by SM synthase (SMSs) and sphingomyelinase (SMase) respectively. The levels of ceramide and SMase increase in the brains of both AD model mice and patients (Jana and Pahan, 2004; Grimm et al., 2011; Dinkins et al., 2016). Ceramide promotes stability of BACE1 (Costantini et al., 2007), the generation and aggregation of Aβ (Geekiyanage and Chan, 2011; Dinkins et al., 2016), thus being taken as a risk factor of AD. Inhibition of neutral SMase2 ameliorates AD pathology and improves cognition in AD transgenic mice through reducing exosome secretion, which is enriched with ceramide (Dinkins et al., 2016).

Sphingomyelin synthases (SMSs), which mainly include SMS1 and SMS2, are the last enzymes in the sphingomyelin (SM) biosynthetic pathway. SMSs use ceramide and phosphatidylcholine (PC) as substrates to produce SM and diacylglycerol (DAG). SMS1 is mainly located in the Golgi apparatus, while most SMS2 resides at the plasma membrane (Tafesse et al., 2006). SMS1 shows a capability to produce higher SM content than SMS2 (Shakor et al., 2011). Overexpression of SMS1/2 increases the levels of SM, DAG and ceramide (Ding et al., 2008). It is worth noting that increased levels of SMS1, but not of SMS2, in the hippocampus of AD patients. Inhibition of SMS using a SMS inhibitor, D609, reduces Aβ levels in culture medium with an unknown mechanism (Hsiao et al., 2013). Moreover, elevated SM levels have been observed in the plasma, cerebrospinal fluid (CSF) and brains of AD patients and showed correlation with amyloid plaques (Pettegrew et al., 2001; Chan et al., 2012; Kosicek et al., 2012; Hsiao et al., 2013). In contrast, some studies have observed decreased SM levels in AD brains (Jana and Pahan, 2004; Yang et al., 2004; Grimm et al., 2005; He et al., 2010). Despite of these conflicting observations, in comparison to ceramide, the function of other sphingolipids such as SM in the etiology of AD remains unknown. Therefore, it is worth investigating that the functions of SMS1 in AD pathogenesis, which may help us understand the roles of SMS1-modulated sphingolipids in AD etiology.

We herein show that knockdown of SMS1 by injecting of AAV8 encoding SMS1 shRNA into the hippocampus of APP/PS1 mice, which overexpress mutant human APP and PS1 (Deng et al., 2016), attenuates AD-like pathology such as accumulation of Aβ, neuroinflammation, loss of synapses and cognitive deficits of these mice. We further observe inhibition or knockdown of SMS1 enhances lysosomal degradation of BACE1. We describe inhibition or knockdown of SMS1 causes BACE1 to distribute less in the Golgi, whereas to accumulate in the early endosomes and lysosomes. Thus, we conclude that inhibition of SMS1 promotes lysosomal degradation of BACE1 through regulating the intracellular trafficking of BACE1.

2. Experimental procedures

2.1. Mice

Mice were housed at the SPF Animal Center of Soochow University at 20 °C with a 12-h light/12-h dark cycle (lights on at 6:00 am and off at 6:00 pm).They were maintained in cages with free access to food and water. Male APP/PS1 transgenic mice that co-express mutant human *APP* and *PS1* (Jackson Laboratory, 004462) were used for behavioral tests. All experiment procedures followed the guideline approved by the Institutional Animal Care and Use Committee of Soochow University. After behavior test, the mice were sacrificed by dislocation, the brains were taken for subsequent sectioning or protein extraction.

2.2. Antibodies

Anti-GAPDH (CMCTAG, USA), anti-Aβ (6E10, Convance, USA), anti-Iba1 (Wako, Japan), anti-BACE1 (CST, USA), anti-SMS1 (Proteintech, USA), anti-lysenin (Peptide Institute, Japan), rat anti-neprilysin (R&D system, USA), Alexa Fluor 555, 488 and 694-conjugated antibodies (Invitrogen, USA). Anti-γ-tubulin, anti-HA, anti-APP and horseradish peroxidase (HRP)-conjugated antibodies were purchased from Sigma (USA). Anti-GFAP, anti-synaptophysin, anti-LAMP1, anti-EEA1, anti-GM130 and anti-IDE were purchased from Abcam (UK).

2.3. Cells and siRNA

HEK293 cells stably expressing BACE1-HA were cultured in medium containing 40 μg/ml hygromycin B. Human SMS1 and SMS2 siRNAs are as following: SMS1 sense: 5'-CUACACUCCCAGUACCUGG-3′; SMS2 sense: 5'-ACCUGUUGCACCGAUAUUCAA-3′.

For BACE1 degradation analysis, HEK293 cells were cotransfected with BACE1-HA and SMS1 siRNA for 12 h, followed by treatment with 40 μg/ml cycloheximide (CHX). The cells were harvested at different time points after treatment.

2.4. AAV vector administration

AAV8, which encodes EGFP under CMV promoter and either scrambled shRNA (NC) or a SMS1 shRNA sequence under U6 promoter were purchased from Heyuan Biotech. Ltd. Co. (Shanghai, China). One microliter of AAV8 (1×10^{13} vg/ml) were injected bilaterally into the dorsal hippocampus (−2.0 mm AP, ± 1.7 mm ML, −2.0 mm DV from bregma) of 4 month-old mice using a stereotaxic apparatus (RWD Life Science, China) via a microprocessor controlled minipump (Longer Pump, UK) at a rate of 0.2 μl/min. Behavioral tests were performed 3 months after AAV8 injection.

2.5. Immunofluorescence staining and quantification

Immunofluorescence staining was performed as described (Zhang et al., 2014; Deng et al., 2016). The quantification of immunofluorescence was performed as described (Zhang et al., 2014). The images were converted into 8-bit images and binarized after subtracting the background noise using NIH Image J software. Mean fluorescence intensities (MFIs) of synaptophysin, GFAP, Iba1 and lysenin was measured and calculated by dividing the MFI units by the area of outlined regions. The intensity threshold was set and kept constant for all images analyzed. The numbers of Aβ plaques per section were counted. The size of Aβ plaques was quantified and expressed as the areas of Aβ plaques being divided by the total areas of the cortex or hippocampus. For quantification, the sections from five mice per group and at least eight hippocampal sections per mouse were analyzed ($n = 5$).

The colocalization between BACE1 and LAMP1/GM130/EEA1 in cultured cells and hippocampal sections was analyzed by Image J by quantifying the Pearson's correlation coefficient. Total 120 cells per group from 4 replicated experiments ($n = 4$) were analyzed. 60–80 amyloid plaques per group of mice (four mice per group, n = 4) were analyzed.

2.6. qRT-PCR analysis

Real time PCRs were carried out with SYBR Green 1 (Roche, Switzerland) using the following primers pairs: human *BACE1* (5′-ACCAACCTTCGTTTGCCCAA-3′; 5′-TCTCCTAGCCAGAAACCATCAG-3′); mouse *BACE1* (5′-GGAACCCATCTCGGCATCC-3′; 5′-TCCGATTCCTCGTCGGTCTC-3′); human *SMS1* (5′-CAGCATCAAGATTAAACCCAACG-3′; 5′-TGGTGAGAACGAAACAGGAAAG-3′); mouse *SMS1* (5′-GAAGGAAGTG GTTTACTGGTCAC-3′; 5′-GACTCGGTACAGTGGGGGT-3′); human *SMS2* (5′-TCCTACGAACACTTATGCAAGAC-3′;

5′-CCGGGTACTTTTTGGTGCCT-3′); human *GAPDH* (5′-GCACCACAAA GCTGCAGGGAGAA-3′; 5′-AATCCGTTGACTCCGACCTTC-3′); mouse *GAPDH* (5′-AGGTCGGTGTGAACGGATTTG-3′; 5′-TGTAGACCATGTAG TTGAGGTCA-3′). Quantification of *BACE1*, *SMS1* and *SMS2* gene expression was carried out by classic 2^ (−△△ Ct) method.

2.7. Analysis of the levels of Aβ by enzyme linked immunosorbent assays (ELISA)

Measurement of soluble and insoluble Aβ were carried out by a two-step protocol. Briefly, in the first step, the cortex and hippocampus were homogenized in 400 μl TBS (20 mM Tris, 137 mM NaCl, pH 7.6) containing protease inhibitors (Roche, Germany). Homogenates were spun at 350, 000 *g* for 30 min at 4 °C. The supernatant, defined as soluble fraction, was collected. In the second step, the pellet was resuspended in 400 μl 5 M guandine (50 mM Tris-HCL, PH 8.0) with protease inhibitors, homogenized for 3 h at RT and centrifuged at 15,000*g* for 10 min at 4 °C. The supernatant, defined as insoluble fraction, was obtained. Soluble and insoluble Aβ were analyzed with human Aβ42 (KHB3441, Invitrogen, USA) and Aβ40 (KHB3481, Invitrogen, USA) ELISA kits according to the manufacturer's instructions.

2.8. Sphingomyelin level measurement and lysenin staining

The measurement of sphingomyelin was performed according to manufacturer's instructions (K600–100, BioVision, USA). In the assay, sphingomyelin is hydrolyzed into ceramide and phosphorylcholine by sphingomyelinase. Alkaline phosphatase (ALP) dephosphorylates phosphorylcholine to choline, which then reacts with Sphingomyelin Enzyme Mix to produce an intermediate. The intermediate reacts with a highly specific probe to generate color (OD 570 nm). Briefly, the mouse hippocampus was homogenized in 0.5 ml of SM Assay Buffer, centrifuged at 4 °C for 5 min at 10,000*g*. The supernatant was diluted by SM Assay Buffer to appropriate proportion and heated for 1–2 min at 70 °C or until it becomes cloudy. After centrifugation at RT for 2 min at 10,000*g*, the supernatant was collected and measured. SM standard curve was made by diluting SM Standard into a series of wells in 96-well plate to generate 0, 1, 2, 3, 4 and 5 nmol/well of SM Standard. Both sample and SM standard were adjusted the volume to 50 μl with SM Assay Buffer, following being added 50 μl reaction buffer and incubated at 37 °C for 1 h. Absorbance (570 nm) was measured in a microplate reader. For lysenin staining, the CHO cells pretreated with D609 for 24 h were fixed with 3% paraformaldehyde in PBS for 20 min at RT. The cells were then blocked with 2% BSA in PBS for 1 h at RT, followed by incubation with 1 μg/ml lysenin (Sigma, USA) with 0.2% BSA in PBS for 1 h. After washing with PBS, the cells were incubated with anti-lysenin antiserum (1:500 with 0.2% BSA in PBS) for 1 h, followed by incubation with Alexa Fluor 488 goat anti-rabbit IgG for 1 h. Fluorescence images were obtained using a Zeiss confocal microscope.

2.9. Novel object recognition

The Novel object recognition (NOR) task was performed as described (Zhang et al., 2014). The recognition index was defined as the percentage of time spent on the novel object to that spent on both objects. The preference index was defined as the percentage of time spent on one of two identical objects to that spent on both objects.

2.10. Morris water maze

Spatial learning and memory was performed in the Morris water maze using procedures similar to those described previously (Zhang et al., 2014). Briefly, each mouse was given four trails daily with a 1 h inter-trial interval. During each trial, mice were allowed to swim until they found the hidden platform where they remained for 8 s before being returned to a holding cage. The trail was ended in 60 s even the mouse did not find the platform. After 5 consecutive days training, the platform was removed and a probe trail was presented. The escape latency, the swimming speed and the number of crossing the position where the platform supposed to be during probe trail, were recorded and analyzed.

2.11. Statistical analysis

All data are presented as mean ± s.e.m. and analyzed using SPSS software. “n” means the numbers of mice per group or the numbers of replicated experiments. Differences between two groups were assessed by two tail t-student test. Comparisons between multiple groups were analyzed by One way ANOVA followed by the Fisher LSD test. Two way ANOVA followed by the Fisher LSD test was only used for escape latency analysis in Morris water maze. All statistical methods used were indicated in the figure legends. Differences were considered statistically significant if $p < 0.05$ (*: $p < 0.05$, **: $p < 0.01$, ***: $p < 0.001$).

3. Results

3.1. Knockdown of SMS1 rescues cognitive deficits of APP/PS1 transgenic mice

To examine the effects of knockdown of SMS1 on AD pathogenesis, we injected AAV8, which encodes both SMS1 shRNA and EGFP, bilaterally into the hippocampus of 4-month-old APP/PS1 transgenic mice, when amyloid plaques appear (Zhang et al., 2014; Deng et al., 2016). As described (Deng et al., 2016), only hippocampal neurons (Fig. 1a), but not microglia (Fig. S1), were infected with AAV8 successfully as indicated by $EGFP^+$ cells. Injection of SMS1 shRNA decreased the levels of SMS1 mRNA and protein in the hippocampus of APP/PS1 mice (Fig. 1b and 1c). Moreover, elevated levels of SM were observed in the hippocampus of APP/PS1 transgenic mice, which were also rescued by knockdown of SMS1 (Fig. 1d). In contrast, the levels of SMS1 in the cortex of SMS1 shRNA-injected APP/PS1 mice, where no AAV8 were injected into, remained unchanged compared to that in NC-injected APP/PS1 transgenic mice (Fig. 1b).

To further examine whether knockdown of SMS1 attenuates the cognitive deficits of APP/PS1 transgenic mice, behavioral tests were performed. In novel object recognition task, APP/PS1 transgenic mice exhibited reduced recognition index compared to wild type (WT) mice, which were rescued by knockdown of SMS1 in the hippocampus (Fig. 1e). The preference index remained similar in each group of mice (Fig. 1f), indicating the reduced recognition index observed was not due to different preference to the objects. In Morris water maze tests, in comparison to WT mice, APP/PS1 transgenic mice exhibited longer escape latencies in the consecutive trials (Fig. 1g), and swam less frequently cross over the target site, where the platform originally located during training phase (Fig. 1h), which were rescued by injection of SMS1 shRNA hippocampally. No difference in swimming speed was observed among three groups of mice (Fig. 1i), excluding the possibility that the differences in escape latencies and frequency of target site cross was due to distinct swimming speed. Therefore, knockdown of SMS1 in the hippocampus rescues cognitive deficits of APP/PS1 mice.

3.2. Knockdown of SMS1 attenuates accumulation of Aβ in APP/PS1 mice

Accumulation of Aβ plays key roles in AD pathogenesis (Musiek and Holtzman, 2015). We thus examined whether knockdown of SMS1 affects Aβ levels. As revealed by Aβ staining, SMS1 shRNA-injected APP/PS1 transgenic mice exhibited decreased numbers and size of amyloid plaques in the hippocampus (Fig. 2a-c). ELISA analysis further showed that the levels of both soluble and insoluble Aβ42 in the hippocampus of APP/PS1 transgenic mice were decreased by SMS1 knockdown (Fig. 2e). Soluble Aβ40 levels also exhibited a tendency of a reduction in the hippocampus of SMS1 shRNA-injected APP/PS1 mice, compared

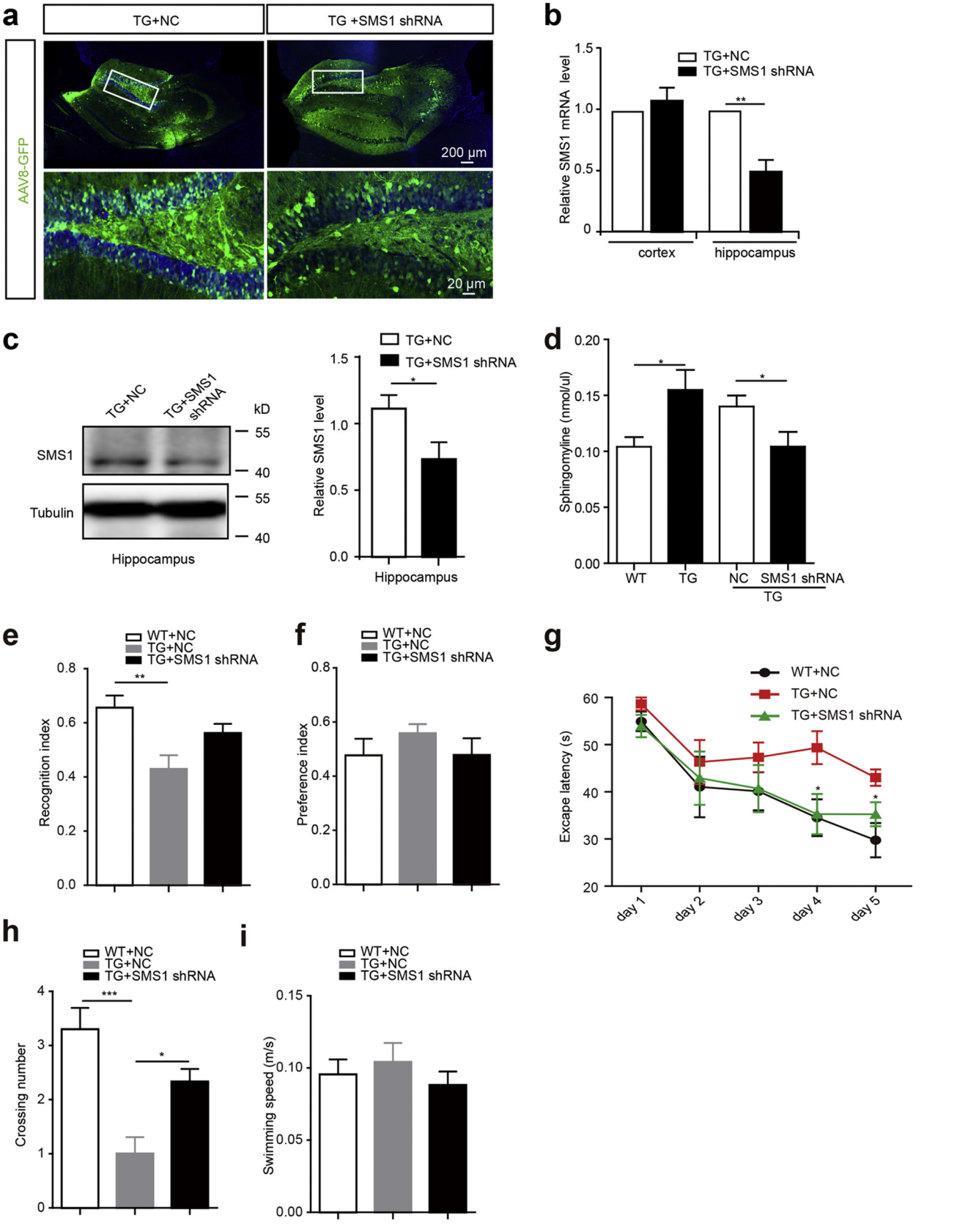

(caption on next page)

Fig. 1. Knockdown of SMS1 ameliorates cognitive deficits of APP/PS1 mice. 4-month-old APP/PS1 transgenic mice were injected with AAV8 encoding SMS1 shRNA or scrambled shRNA (NC) into the hippocampus and maintained for 1–3 months as indicated before sacrifice. WT littermates injected with AAV8-NC as the control. a: GFP^+ fluorescence in the coronal sections of the hippocampus was imaged at 2 months after injection. Scale bar: 200 μm in upper panel and 20 μm in lower panel b: qPCR analysis of the relative levels of SMS1 mRNA in the cortex and ippocampus of SMS1 shRNA- and NC-injected transgenic mice 1 month after injection. The levels of SMS1 mRNA in the cortex and hippocampus of NC-injected transgenic mice were normalized to 1.0 c: Western blot analysis of SMS1 levels in the hippocampus and cortex of virus-injected mice 2 months after injection. d: Analysis of SM levels in the hippocampus of virus-injected mice 2 months after injection e, f: Novel object recognition tests on virus-injected mice 3 months after injection. Recognition index (e) and preference index (f) were analyzed g-i: Morris water maze tests. Escape latencies (g), numbers of platform site crossings during the probe test (h) and average swimming speed (i) were analyzed Results are presented as mean + s.e.m. *: $p < 0.05$; **: $p < 0.01$; ***: $p < 0.001$; $n = 4$–6 mice (b-d) or 11–15 mice/group (e-i), two tail t-student test (b, c), Two way ANOVA followed by the Fisher LSD test (g). One way ANOVA followed by the Fisher LSD test (d-f, h, i).

to that in NC-injected APP/PS1 mice, although no statistical difference was detected between two groups of mice (Fig. 2f). Neither levels of Aβ42/40 (Fig. 2g and h) nor the density of amyloid plaques (Fig. 2a and d) exhibited any difference in the cerebral cortex of two groups of mice, where no AAV8 were injected, further confirming the reduction in amyloid plaque density and Aβ levels in the hippocampus were caused by knockdown of SMS1. Together, these data demonstrate that knockdown of SMS1 reduces accumulation of Aβ in the brains of APP/PS1 transgenic mice.

3.3. Knockdown of SMS1 ameliorates loss of synapses and neuroinflammation in APP/PS1 mice

Loss of synapses is strongly correlated with cognitive decline in AD (Smith et al., 2009; Yan et al., 2016; Mirza and Zahid, 2018). We thus investigated whether SMS1 knockdown ameliorated synaptic loss in the brains of APP/PS1 transgenic mice by staining the hippocampal sections for synaptophysin (SYN), a protein specifically expressed in presynapses and representing synaptic function (Piret et al., 2013). SMS1 shRNA-injected APP/PS1 mice displayed enhanced SYN^+ immunoreactivity in the hippocampal CA3 area where synapses are enriched (Fig. 2i and j), implicating SMS1 knockdown attenuates synaptic loss in APP/PS1 mice.

Neuroinflammation is an essential contributor to AD pathophysiology (Shadfar et al., 2015; Calsolaro and Edison, 2016). To investigate whether SMS1 knockdown ameliorates neuroinflammation, we analyzed the densities of astrocytes and microglia, two types of cells eliciting the inflammatory response in the brains of AD patients and AD model mice (Calsolaro and Edison, 2016), by staining the hippocampal sections for GFAP and Iba-1, which are makers for astrocytes and microglia respectively. Both astrocytes (Fig. 2k and l) and microglia (Fig. 2m and n) exhibited decreased densities in the hippocampus of SMS1 shRNA-injected APP/PS1 mice, indicating that knockdown of SMS1 attenuates neuroinflammation of APP/PS1 transgenic mice.

3.4. Inhibition of SMS1 reduces β-secretase cleavage of APP

Given that knockdown of SMS1 attenuates AD pathology including Aβ accumulation, neuroinflammation, loss of synapses and cognitive deficits. Among them, Aβ is the initiator to trigger all these pathological processes (Musiek and Holtzman, 2015). We therefore investigated the underlying mechanisms for SMS1-regulating Aβ metabolism. SMS1 knockdown does not change the expression of insulin degrading enzyme (IDE) and neprilysin, two enzymes degrading Aβ (Miners et al., 2010) (Fig. S2a-d) suggests that SMS1 may not regulate the clearance of Aβ. We then examined whether knockdown of SMS1 affects the generation of Aβ from the cleavage of APP. The levels of β-CTF (C-terminal fragment of APP), which is produced by cleavage of APP by BACE1, decreased in the hippocampus, but not in the cortex where no SMS1 shRNA were injected into, of SMS1 shRNA-injected APP/PS1 transgenic mice, compared to those in NC-injected transgenic mice (Fig. 3a and b). In contrast, the levels of full-length APP (Fig. 3d and e) and α-CTF (Fig. 3a and c) which is produced by cleavage of APP by α-secretase, remained unchanged in the hippocampus of APP/PS1 transgenic mice upon SMS1 knockdown. Thus, knockdown of SMS1 decreases the cleavage of APP by β-secretase. To further confirm these results, we treated the cultured cells with D609, which inhibits the activity of both SMS1 and SMS2 (Adada et al., 2016). Treatment with D609 decreased SM levels in CHO cells as revealed by reduced fluorescent immunoreactivity of lysenin, a SM-specific binding protein (Fig. 3g and h). D609-treated CHO cells exhibited decreased levels of β-CTF (Fig. 3i and j), rather than α-CTF (Fig. 3i and k) and full-length APP (Fig. 3i and l), compared to control cells. Thus, these results indicate that knockdown or inhibition of SMS decreases the generation of Aβ through suppressing the cleavage of APP by β-secretase. In addition, the ratio of Aβ42/Aβ40, which is altered by γ-secretase cleavage of APP (Borchelt et al., 1996), in the hippocampus of APP/PS1 transgenic mice, was not changed by knockdown of SMS1 (Fig. 3f), indicating that SMS1 does not affect γ-secretase activity.

3.5. SMS1 regulates BACE1 level via a post-transcriptional mechanism

BACE1 is β-secretase in the brains. We then examined whether inhibition of SMS1 reduces Aβ generation by regulating BACE1 expression. Both mature and immature BACE1 levels were decreased by treatment with D609 in a dose-dependent manner in CHO and HEK293 cells, which were transfected with BACE1-HA (Fig. 4a-d). SMS1 has higher capability to catalyzing SM production than SMS2 (Shakor et al., 2011), we thus examined whether these two enzymes have distinct capability in reducing BACE1 levels. The siRNAs targeting SMS1 or SMS2, which reduced mRNA levels of SMS1 by 50% and of SMS2 by 70% respectively (Fig. S3), were transfected to HEK293 cells stably expressing BACE1-HA (HEK293 BACE1-HA). BACE1 showed decreased levels in SMS1 siRNA-transfected cells, and a trend of decreased levels in SMS2 siRNA-transfected cells, although no statistical difference was obtained (Fig. 4e and g). Whereas neither SMS1 siRNA nor SMS2 siRNA alter APP levels (Fig. 4e and f). Moreover, knockdown of both SMS1 and SMS2 together failed to further reduce BACE1 levels compared to knockdown of SMS1 alone (Fig. 4h and i), implicating a dominant role of SMS1 in regulation of BACE1. In contrast, neither SMS1 siRNA nor D609 changed the levels of BACE1 mRNA in both HEK293 cells and CHO cells (Fig. 4j and k). Consistent with these results, the abnormally elevated BACE1 levels in the hippocampus of APP/PS1 transgenic mice was rescued by knockdown of SMS1 (Fig. 4l and m). Thus, these results indicate that inhibition of SMS1 reduces BACE1 expression post-transcriptionally.

3.6. SMS1 affects the intracellular trafficking of BACE1

SMS1 regulates BACE1 expression posttranscriptionally. We thus examined whether SMS1 regulates stability of BACE1. HEK293 cells cotransfected with BACE1-HA and either SMS1 siRNA or its scrambled control siRNA (NC) were treated with cycloheximide (CHX), which is known to block translational elongation (Schneider-Poetsch et al., 2010). BACE1 levels exhibited accelerated declining rate in SMS1 siRNA-transfected cells, compared in NC-transfected cells (Fig. 5a and b), indicating that knockdown of SMS1 reduces BACE1 stability.

SM, which is reduced by knockdown of SMS1, is important for the intracellular trafficking and internalization of proteins through creating lipid rafts (Rushworth and Hooper, 2010; Slotte, 2013). Internalization

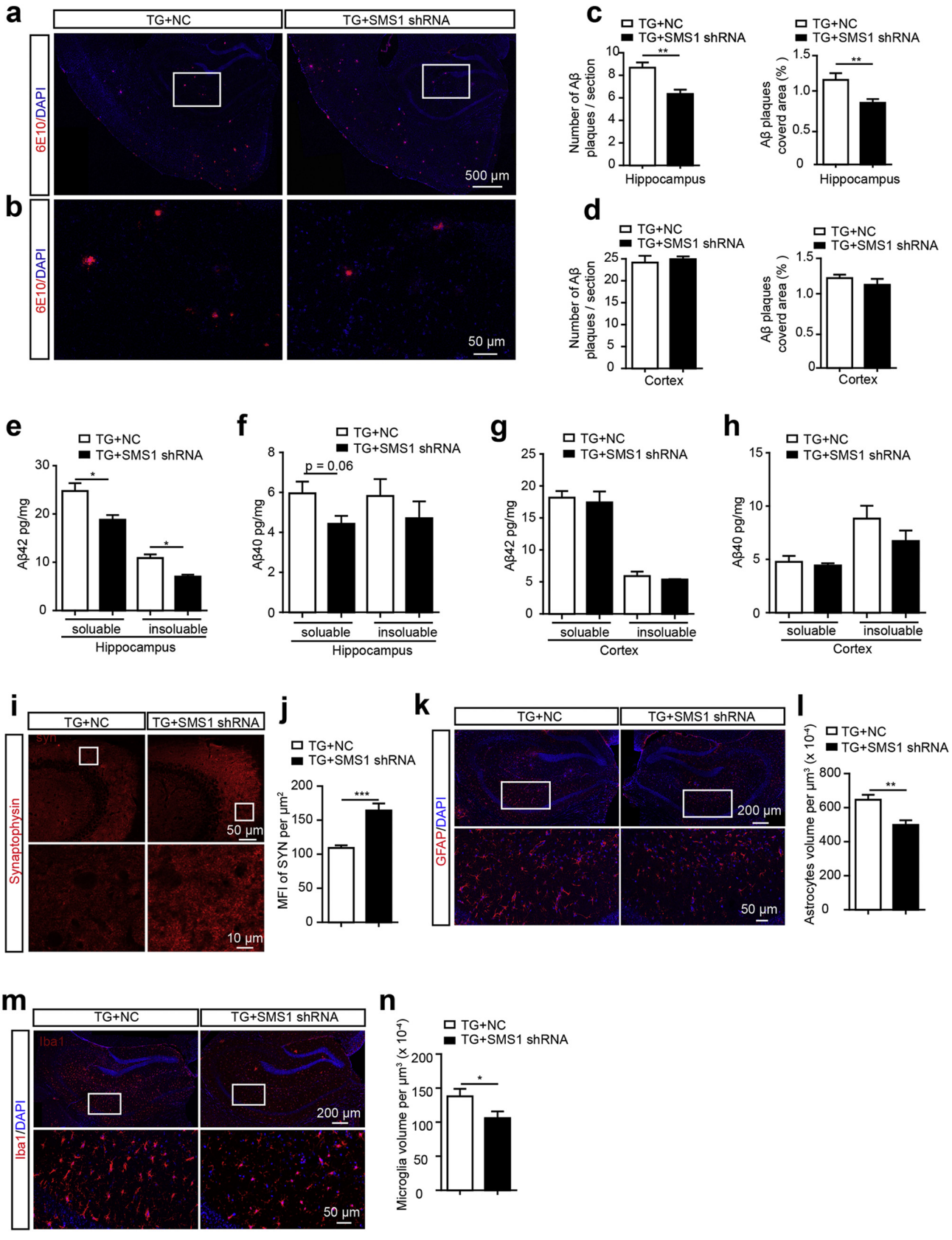

(caption on next page)

Fig. 2. Knockdown of SMS1 reduces accumulation of Aβ, synaptic loss and neuroinflammation 4-month-old APP/PS1 transgenic mice were injected with AAV8 encoding SMS1 shRNA or scrambled shRNA (NC) into the hippocampus and maintained for 3 months before sacrifice. WT littermates injected with AAV8-NC as the control.

a-d: The coronal sections of the cortex and hippocampus of virus-injected APP/PS1 transgenic mice were stained with anti-Aβ antibody (6E10) (a, b). The numbers and the size of amyloid plaques in the hippocampus (c) and the cortex (d) of virus-injected mice were quantified. Scale bars: 500 μm in a and 200 μm in b. e-h: ELISA analysis of the levels of soluble and insoluble Aβ42 (e, g) and Aβ40 (f, h) in the hippocampus and the cortex of virus-injected APP/PS1 transgenic mice. i, k and m: The coronal sections of the hippocampus were stained for synaptophysin (SYN, i), GFAP (k), Iba-1 (m) and DAPI (k, m). The lower panels of i, k and m represent the enlarged view of white boxes in corresponding upper panels. The mean fluorescence intensities (MFI) of SYN^+ immunoreactivity in the CA3 area were analyzed (j). The densities of astrocytes (l) and microglia (n) were analyzed and expressed as the volume per 10^{-4} μm^3. Scale bars: 50 μm (upper, i) and 10 μm (lower, i), 200 μm (upper, k, m) and 50 μm (lower, k, m). Results are presented as mean ± s.e.m. *: $p < 0.05$; **: $p < 0.01$; ***: $p < 0.001$; two tail t-student test. $n = 5$ mice/group.

of BACE1 from the plasma membrane is important for maintenance its stability. Impairing endocytosis by mutating the dileucine motif ($LL^{499/500}$) in BACE1 into alanine ($BACE1_{LLAA}$ mutant) can increase BACE1 stability through retaining BACE1 on the plasma membrane (Kang et al., 2012). We thus wondered whether knockdown of SMS1 regulates BACE1 stability in a way dependent on its endocytosis. However, the levels of $BACE1_{LLAA}$ mutant, similar to WT BACE1 ($BACE1_{WT}$), were reduced by knockdown of SMS1 (Fig. S4a and b), indicating that SMS1 regulate BACE1 expression in a way independent on endocytosis of BACE1. The nascent BACE1 is acetylated on the seven lysine residues of its N-terminal portion, which is required for translocation of the nascent protein from the ER to the secretory pathway and thus controlling BACE1 stability (Costantini et al., 2007). $BACE1_{Ala}$ mutant, in which the seven lysines of BACE1 ($K^{126, 275, 279, 285, 299, 300, 307}$) were mutated to alanines and thus impairing acetylation of BACE1, behaves as "loss of function". Whereas $BACE1_{Gln}$ mutant acts as "gain of function", in which the seven lysine residues were mutated to glutamines, which mimic the effect of lysine acetylation (Costantini et al., 2007). $BACE1_{Ala}$ mutant fails to be exported to the secretory pathway from the ER, whereas $BACE1_{Gln}$ is promoted to be exported from the ER and enhanced its levels on the plasma membrane (Costantini et al., 2007). To examine whether SMS1 regulate BACE1 stability dependent on its acetylation, HEK293 cells were cotransfected with either $BACE1_{Ala}$ mutant or $BACE1_{Gln}$ mutant and SMS1 siRNA. The results showed that knockdown of SMS1 exhibited similar effects in reducing the levels of $BACE1_{wt}$, $BACE1_{Ala}$ and $BACE1_{Gln}$ (Fig. S4c and d). These results indicate that knockdown of SMS1 regulate the stability BACE1 independent on its exportation from the ER. Knockdown of SMS1 decreases BACE1 levels in both the post-Golgi and post-ER compartments.

Most of SMS1 localizes in the trans-Golgi network, where they synthesize SM (Slotte, 2013). We thus examined whether knockdown of SMS1 would change the localization of BACE1 in the Golgi. BACE1-HA transfected HEK293 cells were treated with D609 and coimmunostained for HA and GM130, a marker for Golgi. In control cells which were treated with H_2O, high amount of BACE1 distributed in the perinuclear region and colocalized with GM130. In contrast, BACE1 exhibited diffused punctate pattern (Fig. 5c and e), and decreased colocalization ratio with GM130 in D609-treated cells (Fig. 5c and d), indicating that SMSs inhibition decreases the location of BACE1 in the Golgi. In addition, the colocalization ratio between BACE1-HA and EEA1, a marker of endosomes, increased in D609-treated cells (Fig. 5f and g), indicating that inhibiting SMSs promotes BACE1 to translocate to the endosomes.

3.7. Inhibition of SMS1 promotes degradation of BACE1 via facilitating its translocation to the lysososmes

A small percentage of SM is trafficked to the lysosomes where it is degraded to ceramide by acid SMase (Koval and Pagano, 1990). Considering the observations that SMS inhibition translocates BACE1 into the endosomes, where BACE1 can be degraded after that the endosomes are fused with the lysosomes, we examined whether inhibiting SMSs affects the trafficking of BACE1 to the lysosomes. The colocalization ratio between BACE1-HA and LAMP1, a marker for the lysosome, increased in D609-treated cells, compared to that in H_2O-treated cells, despite in presence or in absence of NH_4Cl, a lysosomal inhibitor (Fig. 6a and b). In AD brains, the lysosomes in dystrophic axons contacting amyloid plaques are dysfunctional, lack of degradative activity and accumulated with BACE1 (Zhao et al., 2007; Gowrishankar et al., 2015). We further observed more BACE1 was accumulated in the dysfunctional lysosomes in the axons adjacent to amyloid plaques upon SMS1 knockdown (Fig. 6c and d). Thus, these results indicate that inhibition of SMSs promotes BACE1 to translocate to the lysosomes. Moreover, in presence of NH_4Cl, a lysosomal inhibitor, D609 failed to reduce BACE1 levels in HEK293 cells (Fig. 6e and f), further indicating inhibition of SMSs decreases BACE1 levels via the lysosomes. Thus, these results indicate that inhibition of SMSs enhances BACE1 to translocate to the lysosomes, where BACE1 is degraded.

4. Discussion

Increased levels of SM have been detected in the CSF and the brains of AD patients (Chan et al., 2012; Hsiao et al., 2013; Kosicek et al., 2012; Mielke et al., 2010), although some studies have reported a contradictory observation (He et al., 2010). The inconstant observation in SM levels in these studies may due to samples from different brain regions, SM species as well as stage of AD symptom development. For instance, high SM levels in the CSF was only observed in prodromal AD (Kosicek et al., 2012). In addition, levels of different SM species also varied even in the same brain regions of AD mouse model (Gonzalez-Dominguez et al., 2014). Despite this inconsistence, the aberrant levels of SM in the brains of AD patients suggest essential roles of SM in AD pathogenesis. We herein describe that knockdown of SMSs, especially SMS1, one of key enzymes in SM synthesis, attenuates accumulation of Aβ, neuroinflammation, loss of synapses and cognitive deficits in APP/PS1 transgenic mice. The present study further shows that inhibition of SMS1 promotes BACE1 to translocate to the lysosomes, where BACE1 is degraded, through modulating the intracellular trafficking of BACE1. Thus, inhibition of SMS1 ameliorates AD pathology through promoting lysosomal degradation of BACE1.

The synthesis of SM is induced by serials of enzymes including serine palmitoyl-CoA transferase (SPT), 3-ketosphinganine reductase, ceramide synthase, dihydroceramide desaturase and SMSs. Among them, SPT is the first enzyme, whereas SMSs being the last enzyme, in the SM biosynthetic pathway (Haughey et al., 2010). SPT is reported as the key enzyme in the biosynthesis of all sphingolipids. However, SMSs are showed as the key enzymes for the biosynthesis of SM. Inhibition or knockdown of SMS1/2 reduces SM levels (Meng et al., 2004; Li et al., 2007; Van der Luit et al., 2007; Ding et al., 2008). Consistent with this result, we indeed observe reduced levels of SM in SMS1-knockdown hippocampus and D609-treated cultured cells. SM is an essential component of membrane lipid rafts. Knockdown of SMS1 reduces the amount of SM in lipid rafts (Van der Luit et al., 2007). Targeting BACE1 to lipid rafts regulates the intracellular trafficking of BACE1 and the cleavage of APP by BACE1 (Zhang and Song, 2013). Thus, a potential mechanism underlying that inhibition of SMS1 promotes lysosomal degradation of BACE1 is that inhibition of SMS1 impairs the localization of BACE1 in the lipid rafts, thus affecting the intracellular trafficking of BACE1 through reducing SM levels.

It is worth noting that inhibition or knockdown of SMS could also

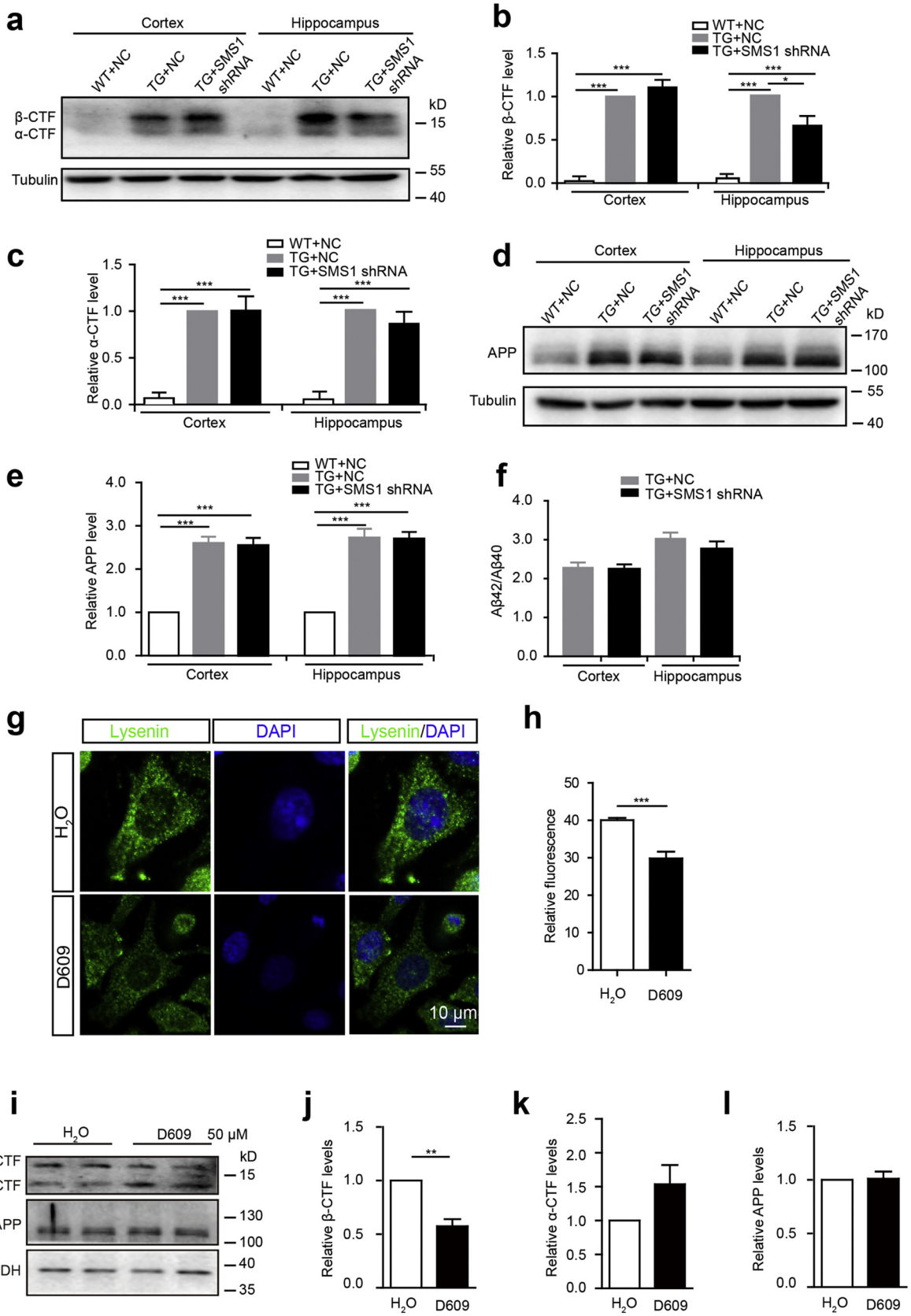

Fig. 3. Knockdown of SMS1 inhibits the cleavage of APP by β-secretase.

a-f: 4-month-old APP/PS1 transgenic mice and WT littermates were injected with AAV8-NC or AAV8-SMS1 shRNA into the hippocampus and maintained for 3 months before sacrifice. Western blotting analysis of the levels of β-CTF (a, b), α-CTF (a, c) and full-length APP (d, e) in the hippocampus and cortex of virus-injected APP/PS1 transgenic mice. The ratio of Aβ42/40 levels in the hippocampus of APP/PS1 transgenic mice detected by ELISA was calculated (f). g, h: CHO cells treated with 50 mM D609 were staining for lysenin (g). Relative fluorescent immunoreactivity was quantified (h). Scale bar: 10 μm. i-l: Western blotting analysis of β-CTF (i, j), α-CTF (i, k) and full-length APP (i, l) in CHO cells treated with 50 μM D609. Results are presented as mean + s.e.m. *: $p < 0.05$; **: $p < 0.01$; ***: $p < 0.001$; One way ANOVA followed by the Fisher LSD test (b, c and e), two tail t-student test (f, h and j-l). n = 4 mice/group (a-f); n = 4 biological repeats (g-l).

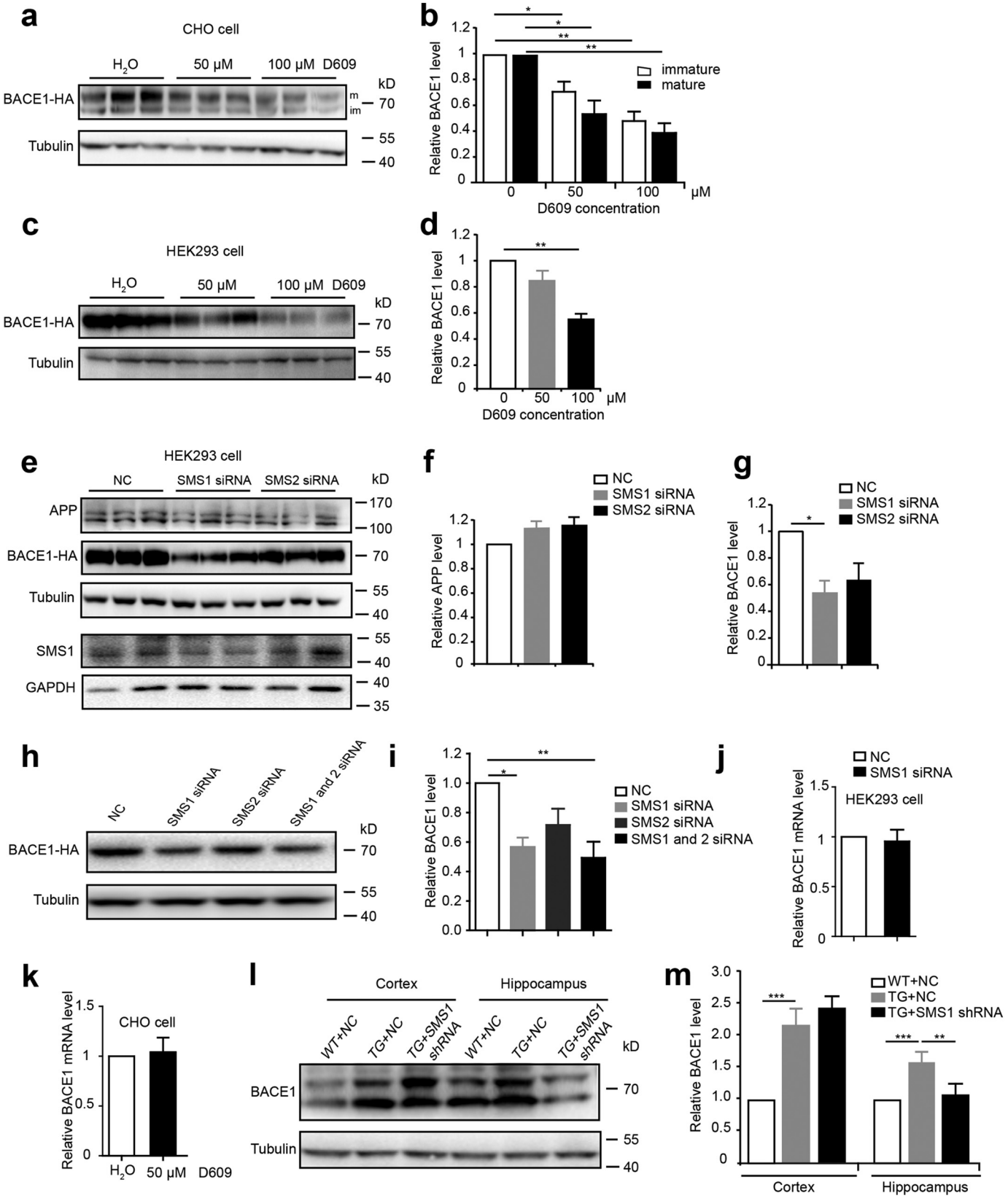

Fig. 4. Knockdown of SMS1 reduces BACE1 levels via a post-transcriptional mechanism.

a-d: Western blotting analysis of BACE1 levels using anti-HA antibodies in CHO (a, b) and HEK293 cells (c, d), which were transfected with BACE-HA and treated with D609. e-i: Western blotting analysis of the levels of BACE1 (e, g, h, i) and APP (e, f) using antibodies against HA and APP, respectively, in HEK 293 cells stably expressing BACE1-HA, which were transfected with siRNA targeting SMS1 or/and SMS2. j, k: qPCR analysis of the levels of BACE1 mRNA in HEK293 cells transfected with SMS1 siRNA (j) or in CHO cells treated with D609 (k). l, m: Western blotting analysis of the levels of BACE1 using antibodies against BACE1 in the hippocampus and cortex of SMS1 shRNA-and NC-injected APP/PS1 mice. Results are presented as mean ± s.e.m. *: $p < 0.05$; **: $p < 0.01$; ***: $p < 0.001$; One way ANOVA followed by the Fisher LSD test (b, d, f, g, i, m), two tail t-student test (j, k). n = 4 biological repeats (b-k) or 4 mice/group (m).

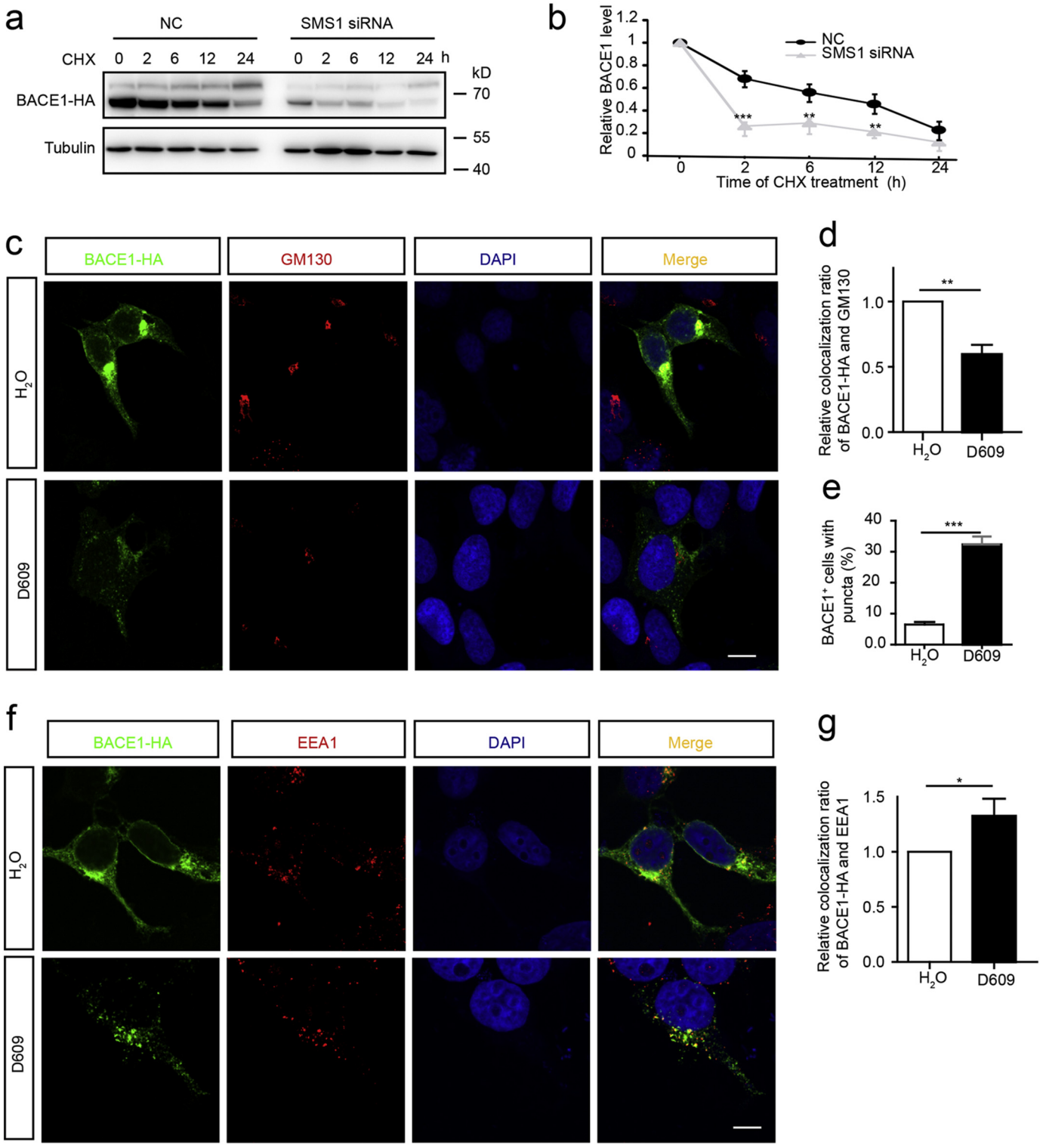

Fig. 5. Inhibition of SMS1 regulates intracellular trafficking of BACE1.
a, b: HEK 293 cells co-transfected with BACE1-HA and SMS1 siRNA were treated with CHX 12 h after transfection. The cell lysates were collected at indicated time after treatment. The levels of BACE1 were analyzed with anti-HA antibodies by Western blotting (a). The levels of BACE1 in SMS1 siRNA- and NC-transfected cells before CHX treatment were normalized to 1.0. The relative levels of BACE1 in the cells treated with CHX for indicated time were analyzed (b). c-g: HEK 293 cells transfected with BACE1-HA were and stained for HA, GM130 (c) or EEA1 (f) and DAPI. The colocalization ratio between HA^+ and $GM130^+$ (d) or $EEA1^+$ (g) fluorescent signals in control cells were normalized to 1.0 for quantification of the relative colocalization ratio. The percentages of cells showing $BACE1^+$ puncta (e). Scale bars: 10 μm. Results are presented as mean + s.e.m. *: $p < 0.05$; **: $p < 0.01$; ***: $p < 0.001$. Two way ANOVA followed by the Fisher LSD test (b); two tail t-student test (d, e, g). $n = 3$–6 biological repeats.

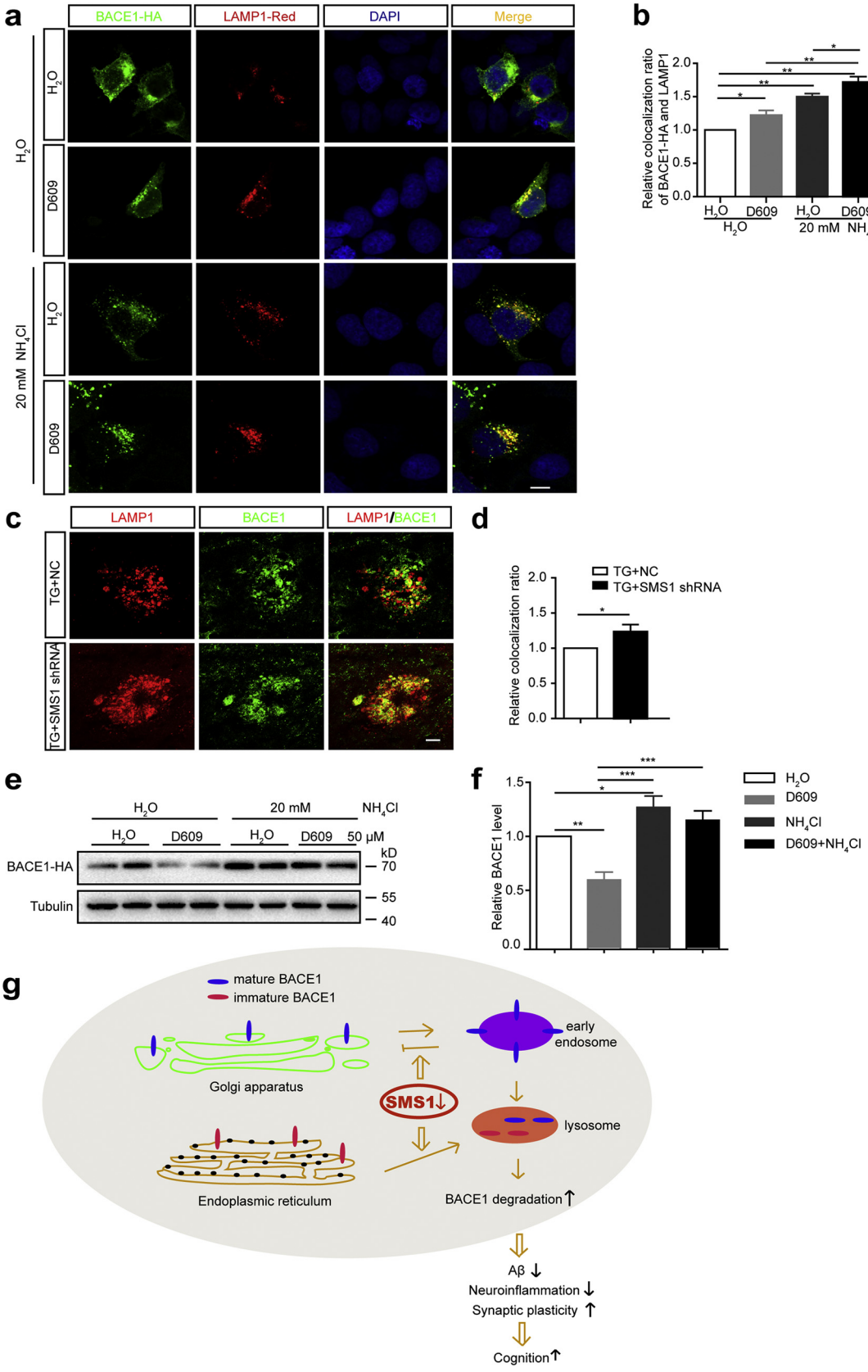

(caption on next page)

Fig. 6. inhibition of SMS promotes BACE1 degradation via the lysosomes.
a, b: HEK 293 cells transfected with BACE1-HA and LAMP1-DsRed were treated with NH_4Cl and stained for HA and DAPI. The colocalization ratio between HA^+ and $LAMP1^+$ fluorescent signals in control cells were normalized to 1.0 for quantification the relative colocalization ratio (i). c, d: The hippocampal sections of SMS1 shRNA-and NC-injected APP/PS1 mice were stained for LAMP1 and BACE1. The colocalization ratio between $BACE1^+$ and $LAMP1^+$ fluorescent signals around amyloid plaques were quantified, while that in control mice were normalized to 1.0 (k). e, f: Western blotting analysis of BACE1 levels using anti-HA antibodies in HEK293 cells stably expressing BACE1-HA, which were treated with 50 μM D609 and NH_4Cl for 24 h. The levels of BACE1 in H_2O-treated cells were normalized to 1.0. g: Schematic description of the effect of knockdown/inhibition of SMS1 on the pathogenesis of AD. Inhibition of SMS1 promotes BACE1 to translocate from the Golgi apparatus to the early endosomes or suppresses BACE1 to translocate retrogradely from the early endosomes to the Golgi apparatus. In either way, knockdown/inhibition of SMS1 promotes BACE1 to translocate to the lysosomes, where BACE1 is degraded. Knockdown/inhibition of SMS1 also promotes the translocation of immature BACE1 from the ER to the lysosomes. Through this way, knockdown/inhibition of SMS1 attenuates elevated BACE1 levels, accumulation of Aβ, neuroinflammation and loss of synapses, eventually improving cognitive function of AD transgenic mice. Scale bars: 10 μm. Results are presented as mean + s.e.m.*: $p < 0.05$; **: $p < 0.01$; ***: $p < 0.001$. One way Anova followed by the Fisher LSD test (b, f); two tail t-student test (d). n = 3–6 biological repeats. n = 4 mice/group (c, d).

lead to decreased DAG levels (Ding et al., 2008). In this context, it is worth noting that D609 is also an inhibitor of phosphatidylcholine-specific phospholipase C (PC-PLC), which PC-PLC hydrolyzes phosphatidylcholine (PC) to generate DAG and phosphocholine (Exton, 1994). DAG is an activator of protein kinase C (PKC) (Nishizuka, 1995). However, in contrast to inhibition of SMS1, which enhances lysosomal degradation of BACE1, PKC, when activated, enhances BACE1 degradation through proteasomes (Wang et al., 2008). Manipulation of SMS alters the cellular levels of ceramide as well. Overexpression of both SMS1 and SMS2 increased the levels of both SM and ceramide (Ding et al., 2008), which may be due to the fact that SMS catalyzes bidirectional reactions between ceramide and SM (Huitema et al., 2004). However, in contrast to overexpression of SMS, knockdown of SMS with siRNA fails to change ceramide levels (Ding et al., 2008). Ceramide promotes BACE1 stability through enhancing its expression on the cell surface, a process dependent on acetylation of BACE1 in the lumen of the ER (Costantini et al., 2007). Consistent with this notion, elevated levels of SMase, which catalyzes SM to generate ceramide, promote Aβ accumulation (Puglielli et al., 2003). Neural SMase2 deficiency ameliorates Aβ plaques burdens and cognitive deficits in 5XFAD transgenic mice, through suppressing exosome-mediated Aβ aggregation (Dinkins et al., 2016). In contrast, our study indicates that inhibition of SMS1 reduces BACE1 stability through promoting BACE1 to translocate to the lysosomes that is independent on both the acetylation and endocytosis of BACE1. Thus, in this context, it seems unlikely that inhibition of SMS1 enhances lysosomal degradation of BACE1 via decreasing ceramide levels. These studies suggest that different metabolites of sphingolipids may play distinct functions in AD pathogenesis. Even ceramide and SM catalytically converse to each other by SMSs and SMase, they may have distinct functions in regulation of BACE1 stability through different molecular mechanisms. It is better to consider the effect of individual SM species and SM/ceramide balance on AD pathogenesis, since reports hint that SM/ceramide ratio may play more important roles in AD cognition (Mielke et al., 2010).

We here show that compared to SMS2, SMS1 has a dominant role in regulating BACE1 levels. Consistent with the fact that SMS1 is mainly localized at the Golgi apparatus, whereas SMS2 mainly functions on the plasma membrane (Slotte, 2013), we observe that SMS1 regulates BACE1 levels independent on its expression on the plasma membrane. This result is also consistent with the observation that SMS1, but not SMS2, increase in the brains of AD patients (Hsiao et al., 2013), where BACE1 levels are upregulated. Inhibition of SMS1 decreases BACE1 levels in the Golgi, whereas increases BACE1 levels in the early endosomes. Since BACE1 can be translocated to the early endosomes from the Golgi and it also can be retrogradely trafficked from the early endosomes to the Golgi (Sun and Zhang, 2017), we here propose that inhibition of SMS1 either suppresses retrograde trafficking of BACE1 from the endosomes to the Golgi or enhances anterograde trafficking of BACE1 from the Golgi to the endosomes (Fig. 6g). However, it remains worth noting that such transiently increased BACE1 in the early endosomes fails to increase Aβ generation. This may be due to the fact that even the proportion of BACE1 in the early endosomes increases upon SMS reduction, the total amount of BACE1 in the early endosomes is still reduced because of lysosomal degradation. It should note that inhibiting SMS levels also decreases immature BACE1, which fails to be exported to the Golgi. Since lysosomal inhibition prevents SMS1 inhibition-reduced both mature and immature BACE1, we propose immature BACE1, which fails to export from the ER, is also translocated to the lysosomes for degradation upon SMS1 inhibition (Fig. 6g).

Sphingolipids play essential roles in neuroinflammation (Gualtierotti et al., 2017). We here observe inhibition of SMS1 reduces neuroinflammation as indicated by reduced densities of both astrocytes and microglia. However, since AAV8 we have used in this study mainly infect neurons, few microglia show being infected by AAV8 (Fig. S1). Thus, the reduced neuroinflammation we have observed in this study may be the secondary change accompanied by reduced generation of Aβ. But we cannot exclude the potential primary roles of SM in neuroinflammation, through which the progression of AD pathogenesis is slowed. Knockdown of SMS specifically in either astrocytes or microglia may help to address this question.

We herein observe that inhibition of SMS1 in neurons attenuates loss of synapses in APP/PS1 transgenic mice, which is consistent with the facts that reduction of SM levels protects cell death (Ding et al., 2008) and that sphingolipids and its metabolites directly modulate synaptic plasticity (Sonnino and Prinetti, 2016). For example, treatment of cells with exogenous gangliosides enhances LTP in the hippocampus (Fujii et al., 2002), whereas impairment of ganglioside synthesis reduces learning ability and other cognitive functions in mice (Sha et al., 2014). However, the attenuation of synaptic loss by inhibition of SMS1 may be also due to decreased levels of Aβ in APP/PS1 transgenic mice. Further investigations in other mouse or cell models may help to answer this question.

Supplementary data to this article can be found online at https://doi.org/10.1016/j.expneurol.2018.09.012.

Disclosure statement

The authors have no conflicts of interest to disclose.

Funding

This work was supported by the National Natural Science Foundation of China (81870897, 81671111, 81601111), Natural Science Foundation of Jiangsu Province, China (BK20181436, BK20150347), Foundation of higher Education of Jiangsu Province, China (15JKB310022), Priority Academic Program Development of Jiangsu Higher Education Institution, China (PAPD), the Suzhou Clinical Research Center of Neurological Disease, China (Szzx201503), Jiangsu Provincial Medical Key Discipline Project, China (ZDXKB2016022) and Jiangsu Provincial Special Program of Medical Science, China (BL2014042) and Jiangsu Key Laboratory of Translational Research and Therapy for Neuro-Psycho-Diseases, China (BM2013003).

Acknowledgements

We thank Dr. Ri-Qiang Yan for providing BACE1-HA plasmid.

References

Adada, M., Luberto, C., Canals, D., 2016. Inhibitors of the sphingomyelin cycle: sphingomyelin synthases and sphingomyelinases. Chem. Phys. Lipids 197, 45–59.
Bertram, L., Tanzi, R.E., 2008. Thirty years of Alzheimer's disease genetics: the implications of systematic meta-analyses. Nat. Rev. Neurosci. 9 (10), 768–778.
Borchelt, D.R., Thinakaran, G., Eckman, C.B., et al., 1996. Familial Alzheimer's disease-linked presenilin 1 variants elevate Abeta1-42/1-40 ratio in vitro and in vivo. Neuron 17 (5), 1005–1013.
Cai, H., Wang, Y., McCarthy, D., et al., 2001. BACE1 is the major beta-secretase for generation of Abeta peptides by neurons. Nat. Neurosci. 4 (3), 233–234.
Calsolaro, V., Edison, P., 2016. Neuroinflammation in Alzheimer's disease: current evidence and future directions. Alzheimers Dement. 12 (6), 719–732.
Chan, R.B., Oliveira, T.G., Cortes, E.P., et al., 2012. Comparative lipidomic analysis of mouse and human brain with Alzheimer disease. J. Biol. Chem. 287 (4), 2678–2688.
Costantini, C., Ko, M.H., Jonas, M.C., et al., 2007. A reversible form of lysine acetylation in the ER and Golgi lumen controls the molecular stabilization of BACE1. J. Biol. Chem. 407 (3), 383–395.
Deng, Q.S., Dong, X.Y., Wu, H., et al., 2016. Disrupted-in-Schizophrenia-1 Attenuates Amyloid-beta Generation and Cognitive Deficits in APP/PS1 Transgenic mice by Reduction of beta-Site APP-Cleaving Enzyme 1 Levels. Neuropsychopharmacology 41 (2), 440–453.
Di Paolo, G., Kim, T.W., 2011. Linking lipids to Alzheimer's disease: cholesterol and beyond. Nat. Rev. Neurosci. 12 (5), 284–296.
Ding, T., Li, Z., Hailemariam, T., et al., 2008. SMS overexpression and knockdown: impact on cellular sphingomyelin and diacylglycerol metabolism, and cell apoptosis. J. Lipid Res. 49 (2), 376–385.
Dinkins, M.B., Enasko, J., Hernandez, C., et al., 2016. Neutral Sphingomyelinase-2 Deficiency Ameliorates Alzheimer's Disease Pathology and Improves Cognition in the 5XFAD Mouse. J. Neurosci. 36 (33), 8653–8667.
Exton, J.H., 1994. Phosphatidylcholine breakdown and signal transduction. Biochim. Biophys. Acta 1212, 26–42.
Foley, P., 2010. Lipids in Alzheimer's disease: a century-old story. Biochim. Biophys. Acta 1801 (8), 750–753.
Fujii, S., Igarashi, K., Sasaki, H., et al., 2002. Effects of the mono- and tetrasialogangliosides GM1 and GQ1b on ATP-induced long-term potentiation in hippocampal CA1 neurons. Glycobiology 12 (5), 339–344.
Geekiyanage, H., Chan, C., 2011. MicroRNA-137/181c regulates serine palmitoyltransferase and in turn amyloid beta, novel targets in sporadic Alzheimer's disease. J. Neurosci. 31 (41), 14820–14830.
Gonzalez-Dominguez, R., Garcia-Barrera, T., Vitorica, J., et al., 2014. Region-specific metabolic alterations in the brain of the APP/PS1 transgenic mice of Alzheimer's disease. Biochim. Biophys. Acta 1842, 2395–2402.
Gowrishankar, S., Yuan, P., Wu, Y., et al., 2015. Massive accumulation of luminal protease-deficient axonal lysosomes at Alzheimer's disease amyloid plaques. Proc. Natl. Acad. Sci. U. S. A. 112 (28), E3699–E3708.
Grimm, M.O., Grimm, H.S., Patzold, A.J., et al., 2005. Regulation of cholesterol and sphingomyelin metabolism by amyloid-beta and presenilin. Nat. Cell Biol. 7 (11), 1118–1123.
Grimm, M.O., Grosgen, S., Rothhaar, T.L., et al., 2011. Intracellular APP Domain Regulates Serine-Palmitoyl-CoA Transferase Expression and is Affected in Alzheimer's Disease. Int. J. Alzheimers Dis. 2011, 695413.
Gualtierotti, R., Guarnaccia, L., Beretta, M., et al., 2017. Modulation of Neuroinflammation in the Central nervous System: Role of Chemokines and Sphingolipids. Adv. Ther. 34 (2), 396–420.
Haughey, N.J., Bandaru, V.V., Bae, M., et al., 2010. Roles for dysfunctional sphingolipid metabolism in Alzheimer's disease neuropathogenesis. Biochim. Biophys. Acta 1801 (8), 878–886.
He, X., Huang, Y., Li, B., et al., 2010. Deregulation of sphingolipid metabolism in Alzheimer's disease. Neurobiol. Aging 31 (3), 398–408.
Holsinger, R.M., McLean, C.A., Beyreuther, K., et al., 2002. Increased expression of the amyloid precursor beta-secretase in Alzheimer's disease. Ann. Neurol. 51 (6), 783–786.
Hsiao, J.H., Fu, Y., Hill, A.F., et al., 2013. Elevation in sphingomyelin synthase activity is associated with increases in amyloid-beta peptide generation. PLoS One 8 (8), e74016.
Huitema, K., van den Dikkenberg, J., Brouwers, J.F., et al., 2004. Identification of a family of animal sphingomyelin synthases. EMBO J. 23 (1), 33–44.
Jana, A., Pahan, K., 2004. Fibrillar amyloid-beta peptides kill human primary neurons via NADPH oxidase-mediated activation of neutral sphingomyelinase implications for Alzheimer's disease. J. Biol. Chem. 279 (49), 51451–51459.
Jonsson, T., Atwal, J.K., Steinberg, S., et al., 2012. A mutation in APP protects against Alzheimer's disease and age-related cognitive decline. Nature 488 (7409), 96–99.
Kang, E.L., Biscaro, B., Piazza, F., et al., 2012. BACE1 protein endocytosis and trafficking are differentially regulated by ubiquitination at lysine 501 and the Di-leucine motif in the carboxyl terminus. J. Biol. Chem. 287 (51), 42867–42880.
Kosicek, M., Zetterberg, H., Andreasen, N., et al., 2012. Elevated cerebrospinal fluid sphingomyelin levels in prodromal Alzheimer's disease. Neurosci. Lett. 516 (2), 302–305.
Koval, M., Pagano, R.E., 1990. Sorting of an internalized plasma membrane lipid between recycling and degradative pathways in normal and Niemann-pick, type a fibroblasts. J. Cell Biol. 111 (2), 429–442.
Li, Z., Hailemariam, T.K., Zhou, H., et al., 2007. Inhibition of sphingomyelin synthase (SMS) affects intracellular sphingomyelin accumulation and plasma membrane lipid organization. Biochim. Biophys. Acta 1771 (9), 1186–1194.
Luo, Y., Bolon, B., Kahn, S., et al., 2001. Mice deficient in BACE1, the Alzheimer's beta-secretase, have normal phenotype and abolished beta-amyloid generation. Nat. Neurosci. 4 (3), 231–232.
Meng, A., Luberto, C., Meier, P., et al., 2004. Sphingomyelin synthase as a potential target for D609-induced apoptosis in U937 human monocytic leukemia cells. Exp. Cell Res. 292 (2), 385–392.
Mielke, M.M., Bandaru, V.V., McArthur, J.C., et al., 2010. Disturbance in cerebral spinal fluid sphingolipid content is associated with memory impairment in subjects infected with the human immunodeficiency virus. J. Neuro-Oncol. 16 (6), 445–456.
Miners, J.S., van Helmond, Z., Kehoe, P.G., et al., 2010. Changes with age in the activities of beta-secretase and the Abeta-degrading enzymes neprilysin, insulin-degrading enzyme and angiotensin-converting enzyme. Brain Pathol. 20 (4), 794–802.
Mirza, F.J., Zahid, S., 2018. The Role of Synapsins in Neurological Disorders. Neurosci. Bull. 34 (2), 349–358.
Musiek, E.S., Holtzman, D.M., 2015. Three dimensions of the amyloid hypothesis: time, space and 'wingmen'. Nat. Neurosci. 18 (6), 800–806.
Naj, A.C., Jun, G., Beecham, G.W., et al., 2011. Common variants at MS4A4/MS4A6E, CD2AP, CD33 and EPHA1 are associated with late-onset Alzheimer's disease. Nat. Genet. 43 (5), 436–441.
Nishizuka, Y., 1995. Protein kinase C and lipid signaling for sustained cellular responses. FASEB J. 9, 484–496.
Pettegrew, J.W., Panchalingam, K., Hamilton, R.L., et al., 2001. Brain membrane phospholipid alterations in Alzheimer's disease. Neurochem. Res. 26 (7), 771–782.
Piret, G., Perez, M.T., Prinz, C.N., 2013. Neurite outgrowth and synaptophysin expression of postnatal CNS neurons on GaP nanowire arrays in long-term retinal cell culture. Biomaterials 34 (4), 875–887.
Puglielli, L., Ellis, B.C., Saunders, A.J., et al., 2003. Ceramide stabilizes beta-site amyloid precursor protein-cleaving enzyme 1 and promotes amyloid beta-peptide biogenesis. J. Biol. Chem. 278 (22), 19777–19783.
Rushworth, J.V., Hooper, N.M., 2010. Lipid Rafts: linking Alzheimer's Amyloid-beta Production, Aggregation, and Toxicity at Neuronal Membranes. Int. J. Alzheimers Dis. 2011, 603052.
Schneider-Poetsch, T., Ju, J., Eyler, D.E., et al., 2010. Inhibition of eukaryotic translation elongation by cycloheximide and lactimidomycin. Nat. Chem. Biol. 6 (3), 209–217.
Sha, S., Zhou, L., Yin, J., et al., 2014. Deficits in cognitive function and hippocampal plasticity in GM2/GD2 synthase knockout mice. Hippocampus 24 (4), 369–382.
Shadfar, S., Hwang, C.J., Lim, M.S., et al., 2015. Involvement of inflammation in Alzheimer's disease pathogenesis and therapeutic potential of anti-inflammatory agents. Arch. Pharm. Res. 38 (12), 2106–2119.
Shakor, A.B., Taniguchi, M., Kitatani, K., et al., 2011. Sphingomyelin synthase 1-generated sphingomyelin plays an important role in transferrin trafficking and cell proliferation. J. Biol. Chem. 286 (41), 36053–36062.
Slotte, J.P., 2013. Biological functions of sphingomyelins. Prog. Lipid Res. 52 (4), 424–437.
Smith, D.L., Pozueta, J., Gong, B., et al., 2009. Reversal of long-term dendritic spine alterations in Alzheimer disease models. Proc. Natl. Acad. Sci. U. S. A. 106 (39), 16877–16882.
Sonnino, S., Prinetti, A., 2016. The role of sphingolipids in neuronal plasticity of the brain. J. Neurochem. 137 (4), 485–488.
Sun, M., Zhang, H., 2017. Par3 and aPKC regulate BACE1 endosome-to-TGN trafficking through PACS1. Neurobiol. Aging 60, 129–140.
Tafesse, F.G., Ternes, P., Holthuis, J.C., 2006. The multigenic sphingomyelin synthase family. J. Biol. Chem. 281 (40), 29421–29425.
Van der Luit, A.H., Budde, M., Zerp, S., et al., 2007. Resistance to alkyl-lysophospholipid-induced apoptosis due to downregulated sphingomyelin synthase 1 expression with consequent sphingomyelin- and cholesterol-deficiency in lipid rafts. Biochem. J. 401 (2), 541–549.
van Echten-Deckert, G., Walter, J., 2012. Sphingolipids: critical players in Alzheimer's disease. Prog. Lipid Res. 51 (4), 378–393.
Walter, J., van Echten-Deckert, G., 2013. Cross-talk of membrane lipids and Alzheimer-related proteins. Mol. Neurodegener. 8, 34.
Wang, L., Shim, H., Xie, C., et al., 2008. Activation of protein kinase C modulates BACE1-mediated beta-secretase activity. Neurobiol. Aging 29 (3), 357–367.
Yan, R., Fan, Q., Zhou, J., et al., 2016. Inhibiting BACE1 to reverse synaptic dysfunctions in Alzheimer's disease. Neurosci. Biobehav. Rev. 65, 326–340.
Yang, L.B., Lindholm, K., Yan, R., et al., 2003. Elevated beta-secretase expression and enzymatic activity detected in sporadic Alzheimer disease. Nat. Med. 9 (1), 3–4.
Yang, D.I., Yeh, C.H., Chen, S., et al., 2004. Neutral sphingomyelinase activation in endothelial and glial cell death induced by amyloid beta-peptide. Neurobiol. Dis. 17 (1), 99–107.
Yang, A., Wang, C., Song, B., et al., 2017. Attenuation of beta-Amyloid Toxicity in Vitro and in Vivo by Accelerated Aggregation. Neurosci. Bull. 33 (4), 405–412.
Zhang, X., Song, W., 2013. The role of APP and BACE1 trafficking in APP processing and amyloid-beta generation. Alzheimers Res. Ther. 5 (5), 46.
Zhang, M.Y., Zheng, C.Y., Zou, M.M., et al., 2014. Lamotrigine attenuates deficits in synaptic plasticity and accumulation of amyloid plaques in APP/PS1 transgenic mice. Neurobiol. Aging 35 (12), 2713–2725.
Zhao, J., Fu, Y., Yasvoina, M., et al., 2007. Beta-site amyloid precursor protein cleaving enzyme 1 levels become elevated in neurons around amyloid plaques: implications for Alzheimer's disease pathogenesis. J. Neurosci. 27 (14), 3639–3649.